Synthesis of Nano-dispersed TiO_2 Zirconium Based Alloy by Mechanical Alloying

A THESIS SUBMITTED IN PARTIAL FULLFILLMENT

OF THE REQUIREMENT FOR THE DEGREE OF

Bachelor of Technology

In

Metallurgical and Materials Engineering

By

RAJAN HORO (109MM0442)

SUDHIR KUMAR DASH (109MM0469)

DEPARTMENT OF METALLURGICAL AND MATERIALS ENGINEERING

NATIONAL INSTITUTE OF TECHNOLOGY, ROURKELA

May, 2012

National Institute of Technology

Rourkela

CERTIFICATE

This is to certify that the thesis entitled "**Synthesis of Nano-dispersed TiO_2 Zirconium Based Alloy by Mechanical Alloying**" being submitted by **Rajan Horo** (109MM0442) and **Sudhir Kumar Dash** (109MM0469) for the partial fulfillment of the requirements of **Bachelor of Technology** degree in **Metallurgical and Materials engineering** is a bona fide thesis work done by them under my supervision during the academic year 2012-2013, in the Department of Metallurgical and Materials Engineering, **National Institute of Technology Rourkela, India**.

The results presented in this thesis have not been submitted elsewhere for the award of any other degree or diploma.

Date:

(Prof. Swapan Kumar Karak)

Metallurgical and Materials Engineering

National Institute of Technology
Rourkela

Rourkela – 769008

ACKNOWLEDGEMENT

We would like to thank **NIT Rourkela** for giving us the opportunity to use its resources and work in such a challenging environment.

First and foremost we take this opportunity to express our immense gratitude to our project guide **Prof. Swapan Kumar Karak**, Department of Metallurgical and Materials Engineering for his able guidance during our project work. This project would not have been possible without his help and valuable time that he has given us.

We would also like to extend our gratitude to **Prof. B.C. Ray**, Head of Department, Metallurgical and Materials Engineering, who has always encouraged and supported us in doing our wok.

Last but not the least; we would like to thank the technical assistants of Metallurgical Department and my friends who helped me directly and indirectly to complete this project successfully.

Finally our cordial thanks to **Mr Mohan Nuthalapati,** PhD scholar who helped us during the period.

Date:

Rajan Horo (109MM0442)

Sudhir Kumar Dash (109MM0469)

Dept. of Metallurgical and Materials Engineering

National Institute of Technology, Rourkela

Rourkela-769008

ABSTRACT

The present work aims to improve the mechanical properties of Zr- alloy (Fe-30-Ni-20-Mo-4 TiO_2-2-Zr-44) (all are in wt. %) synthesized by mechanical alloying and consolidated by conventional sintering. A uniform dispersion of TiO_2 tends to improve the mechanical properties of the present alloys. The current alloys show improvement of hardness value which is 1-1.5 times higher than that of the conventional zircaloy. For this purpose, pure elemental powders of Zr, Ni, Fe, Mo and TiO_2 were blended and milled in a planetary ball mill for 20 h and sintered at 1400°C for 2 h in argon atmosphere. Phase evolution of milled powders at different stages of milling (0h, 1h, 5h, 10h, 15h and 20h) and after sintering of the current alloy were analyzed by X- ray diffraction techniques. The grain morphology or crystallite size of various stages of milled powders was characterized by scanning electron microscope. The crystallite size, lattice strain and lattice parameters were analyzed by Williamson-Hall method. The crystallite size decreases rapidly up to 5hours of milling and becomes almost constant with further milling. Addition of TiO_2 (2 wt %) in the matrix improves the hardness. This is due to the high modulus of elasticity of TiO_2.

Contents

List of Figures

List of Tables

CHAPTER 1

INTRODUCTION

1. Introduction:

In order to acquire amorphous phase the alloys have been treated by different non equilibrium processing techniques such as solid state quenching, rapid solidification, mechanical cold work, irradiation/ion implantation, condensation from vapor and the amorphous powders can be formed by the high energy deformation processing via mechanical alloying[1]. A new generation of Zr based alloys shows amorphorization at much lower cooling rates and high glass forming ability [2]. The excellent chemical, thermal and mechanical properties like high corrosion resistance, less linear coefficient of thermal expansion and high yield strength of zirconium alloy are of great importance since they have high technological impacts in industry [4]. Recently, zirconium based alloys have been huge technological interests for high temperature applications in nuclear reactors or thermal power plants due to its superior thermal stability, excellent high temperature corrosion resistant and stability under radiation or swelling in nuclear environment [5].Zirconium alloys are currently employed in pressurized-water reactors (PWRs) and for the hotter, more highly irradiated structures.

Mechanical alloying is a unique process for fabrication of several alloys and advanced materials at room temperature. MA is a technique for processing of powder in a high-energy ball mill. Originally it was developed to produce oxide-dispersion strengthened Ni- and Fe-based super alloys for application in aerospace industry [1]. MA has capable of synthesizing a variety of equilibrium and non-equilibrium phases starting from blended elemental or pre alloyed powders. Mechanical alloying techniques involved the formation of the non-equilibrium phases, supersaturated solid solutions, metastable crystalline and quasi crystalline phases, nano structures and amorphous alloys [6].

Zirconium alloys are used in the nuclear industry for cladding fuel elements since it has a low absorption cross section of thermal neutrons, high hardness, ductility and corrosion resistance. The oxide in Zirconium is used for laboratory crucibles that will withstand heat shock. The previous experiments tell the elevated temperature yield strength of Zircaloy-2 was increased by dispersion of Y_2O_3 and the absence of tin in M5 (<100 ppm) contributes greatly to its low corrosion rate. This problem was limited by Nano TiO_2 dispersion in zirconium alloys. In

this section we will develop zirconium based alloys by Mechanical alloying with different milling time by dispersion of TiO_2 for Ultra high strength [7].

1.1 Objectives of the Present Piece of Investigation:

- Synthesis of zirconium based alloy (Fe-30-Ni-20-Mo-4-TiO_2-2-Zr-44) (all are in wt. %), by high energy ball milling at different milling time.
- Determine optimum synthesis conditions- [Type of mills (e.g., high-energy mills and low-energy mills), The materials of milling tool (e.g., ceramics, stainless steel, and tungsten carbide), Types of milling media (e.g., balls or rods), Milling atmosphere (e.g., air, nitrogen, and an inert gas), Milling environment (e.g., dry milling or wet milling), Milling media-to-powder weight ratio, Milling temperature, Milling time].
- To study the phase evolution of the mechanically alloyed powders at different stages of milling (0h, 1h, 5h, 10h, 15h and 20h)as well as consolidated alloys using XRD.
- To or apparent study grain morphology crystallite size of the microstructure mechanically alloyed powders at different stages of milling (0h, 1h, 5h, 10h, 15h and 20h) by using SEM.
- To calculate and compare the grain size, lattice strain of milled powders.
- To study hardness property of current alloy.

CHAPTER 2

LITERATURE SURVEY

2. Literature Survey:

2.1 Zircaloy:

Zirconium based alloy is a high temperature refractory alloy with excellent corrosion resistance, good mechanical properties, less exposure to neutron flux, and can be manufactured using standard fabrication techniques. Zirconium alloys are good to improve corrosion resistance and high compressive stresses due to the oxide dispersion. Zirconium has a hexagonal packing structure (α-phase) which transforms into a body centered cubic structure (β phase) above this temperature. It is impossible to obtain this β-phase at room temperature with any type of heat treatment [7]. In this situation the solid state powder processing techniques are of favorable consideration. In this situation mechanical alloying has proven as the preferable process for to produce oxide-dispersion strengthened zirconium alloys [6]. Zirconium is a unique material whose specific weight lies between that of titanium and stainless steel. No metal or alloy is resistant to corrosive attack in all chemical environments. Zirconium is no exception, but it does have excellent resistance to a wide variety of chemicals. Zirconium shows excellent corrosion resistance to all concentrations of hydrochloric acid even at temperatures exceeding the normal boiling point [8]. Zirconium alloys have superior thermal properties compared to other traditional materials in consideration for spent nuclear fuel containers. Zirconium alloys have a thermal conductivity more than 30% higher than stainless steel alloys. The linear coefficient of thermal expansion for Zirconium alloys is nearly one-third the value for stainless steel giving zirconium alloys superior dimensional stability at elevated temperatures [9].

2.1.1 Disadvantages of Zircaloy:

One disadvantage of metallic zirconium is that zirconium cladding rapidly reacts with water steam at high temperature. Oxidation of zirconium by water is accompanied by release of hydrogen gas. This oxidation is accelerated at high temperature [10].

$$\mathbf{Zr + 2\ H_2O \rightarrow ZrO_2 + 2\ H_2}$$

5–20% of hydrogen diffuses into the zirconium alloy cladding forming zirconium hydrides. The hydrogen production process also mechanically weakens the rods cladding

because the hydrides have lower hardness, ductility and density than zirconium or its alloys, and thus blisters and cracks form upon hydrogen accumulation. This process is also known as hydrogen embrittlement [15, 16].

The low temperature hexagonal (α) zirconium phase has a very low solubility of hydrogen, resulting in any excess hydrogen getting precipitated as zirconium hydride. This leads to embrittlement, delayed hydride cracking (DHC) and hydride blistering.

2.1.2 Addition of Alloying Elements:

Alloying elements are able to promote the formation of the α-phase or the β-phase with Zirconium is also known as α- or β-stabilizers. Elements that promote the α-phase include aluminum, antimony, tin, beryllium, hafnium, nitrogen, oxygen and cadmium. Stabilizers that promote the β-phase include iron, chromium, nickel, molybdenum, copper, niobium, tantalum, vanadium, uranium, titanium, manganese, cobalt and silver. Due to the hexagonal structure, values such as the expansion coefficient, tensile strength, elasticity and bending strength vary depending on the orientation of the crystal lattice [20-22].

2.1.3 Advantage of Amorphous Structure:

The atomic structure is the most striking characteristic of the amorphous alloy as it fundamentally differentiates amorphous alloy from ordinary metals. Amorphous metallic alloys are metals and metal alloys with no long range atomic order. They have also been called glassy alloys or non-crystalline alloys. Structure and constitution of advanced material can be better controlled by processing them under non-equilibrium conditions. The theme of the mechanical alloying process is to synthesize materials in non-equilibrium state by energizing and quenching [13].

2.1.4 Applications of Zircaloy:

Zirconium alloys are corrosion resistant and biocompatible, and therefore can be used for body implants. In one particular application, a Zr-2.5Nb alloy is formed into a knee or hip implant and then oxidized to produce a hard ceramic surface for use in bearing against a polyethylene component. This oxidized zirconium alloy material provides the beneficial surface

properties of a ceramic (reduced friction and increased abrasion resistance), while retaining the beneficial bulk properties of the underlying metal (manufacturability, fracture toughness, and ductility), providing a good solution for these medical implant applications [19, 20].

2.2 Mechanical Alloying:

Mechanical alloying is a materials-processing method that involves the repeated welding, fracturing, and rewelding of a mixture of powder particles, generally in a high-energy ball mill, to produce a controlled, extremely fine microstructure. The mechanical alloying technique allows alloying of elements that are difficult or impossible to combine by conventional melting methods [1]. It is a fundamentally different approach to alloy manufacture than traditional techniques which use heat treatments and chemical reactions to combine alloy components as it mainly relies on deformation processes to mix materials. So, deformation taking place is an integral part of the MA process. MA has now been shown to be capable of synthesizing a variety of equilibrium and non-equilibrium alloy phases starting from blended elemental or prealloyed powders [6]. The non-equilibrium phases synthesized include supersaturated solid solutions, metastable crystalline and quasicrystalline phases, nanostructures, and amorphous alloys. MA started as an industrial necessity in 1966 to produce oxide dispersion strengthened (ODS) nickel- and iron-based superalloys for applications in the aerospace industry. MA is a completely solid-state processing technique and therefore limitations imposed by phase diagrams do not apply here[6].

Important milestones in the development of mechanical alloying

- 1966 Development of ODS nickel-base alloys
- 1981 Amorphization of intermetallic
- 1982 Disordering of ordered compounds
- 1983 Amorphization of blended elemental powder mixtures
- 1987/88 Synthesis of nanocrystalline phases
- 1989 Occurrence of displacement reactions
- 1989 Synthesis of quasicrystalline phases

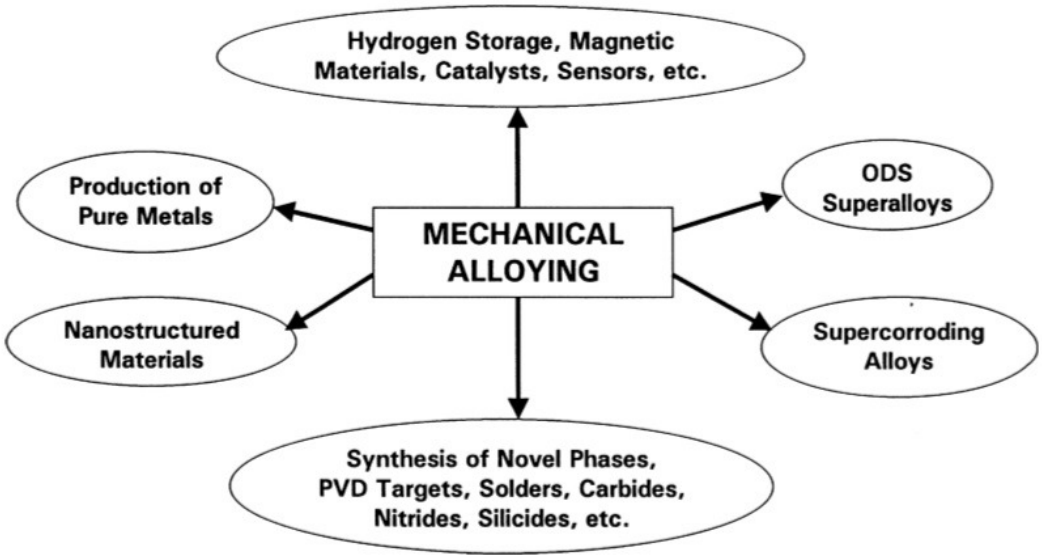

2.2.1 Ability of Mechanical Alloying in the Production of Nano Sturctured Materials:

The ability of the different processing techniques to synthesize metastable structures can be evaluated by measuring the departure from equilibrium, i.e., the maximum energy that can be stored in excess of that of the equilibrium/stable structure. Departure from equilibrium achieved in different non-equilibrium processing techniques [6]. Those are given below

Table 2.1: Different non-equilbrium processing technique

Sl.no	Technique	Technique Effective quencing rate (K/s)	Maximum departure from equilibrium (Kj/mol)
1.	Solid state quench	10^3	16
2.	Rapid solidification	10^5-10^8	24
3.	Mechanical alloying	-	30
4.	Mechanical cold work	-	1
5.	Irradiation/ion implantation	10^{12}	30
6.	Condenssation from vapour	10^{12}	160

2.2.2 Attributes of Mechanical Alloying:

- Production of fine dispersion of second phase (usually oxides like Y_2O_3, TIO_2) particles
- Extension of solid solubility limits
- Refinement of grain sizes down to nanometer range
- Synthesis of novel crystalline and quasicrystalline phases
- Development of amorphous (glassy) phases
- Disordering of ordered intermetallics
- Possibility of alloying of difficult to alloy elements
- Inducement of chemical (displacement) reactions at low temperatures

2.3 Components of MA:

- Raw Materials
- Mill variables
- Process variables

2.3.1 Raw Materials:

Generally raw materials with particle sizes in the range of 1-200μm are used for MA. Ductile-ductile, ductile-brittle and brittle-brittle powder mixtures are milled to produce novel alloys.

The powder particle size decreases exponentially with time and reaches a small value of a few microns only after a few minutes of milling. So, powder particle size is not very critical, except that it should be smaller than the grinding ball size. The raw powders fall into the broad categories of pure metals, master alloys, pre-alloyed powders and refractory compounds. Dispersion strengthened materials usually contain additions of carbides, nitrides, and oxides.

Oxides are the most common and these alloys are known as oxide-dispersion strengthened (ODS) materials. Oxide dispersion improves mechanical properties [1, 6].

2.3.2 Mill Variables:

Mechanical alloying is a complex process and hence involves optimization of a number of variables to achieve the desired product phase. Some of the important parameters that have an effect on the final constitution of the powder are:

- Type of mill
- Milling container
- Milling speed and time
- Type, size, and size distribution of the grinding medium
- Ball-to-powder weight ratio
- Milling atmosphere
- Temperature
-

But, all the process variables mentioned above are not completely independent. For example, the optimum milling time depends on the type of mill, size of the grinding medium, temperature of milling, ball-to-powder ratio, etc [1, 6].

2.3.2.1 Types of Mill:

Different types of high-energy milling equipment are used to produce mechanically alloyed powders. They differ in their capacity, efficiency of milling and additional arrangements for cooling, heating [1]. Those are as follows

- SPEX shaker mills
- Planetary ball mills
- Attrition mills
- Commercial mills

SPEX shaker mills- Which mill about 10±20 g of the powder at a time are most commonly used for laboratory investigations and for alloy screening purposes.

Planetary ball mills- In which a few hundred grams of the powder can be milled at a time. Sample weight is up to 4x250 g.

Attritor mills- Attritors are the mills in which large quantities of powder (0.5 to 40kg) can be milled at a time.

Commercial mills- Commercial mills for MA are much larger in size than the mills described above and can process several hundred pounds at a time. Mechanical alloying for commercial production is carried out in ball mills of up to about 1250 kg capacity.

Table 2.2: Typical capacities of the different types of mills

Sl.no.	Mill type	Sample weight
1.	Mixer mills	Upto 2×20g
2.	Planetary mills	Upto 4×250g
3.	Attritors	0.5-100g
4.	Uni-ball mill	Upto 4×2000g

2.3.2.2 Milling Container:

It is also known as grinding vessel, vial, jar or bowl. During the process of grinding the grinding medium constantly strike on the inner walls of the container and thus can dislodge some material which may join the powder phase. This may contaminate the powder and alter the chemistry of the powder. Some of the common materials used for the grinding vessels are Hardened steel, tool steel, hardened Chromium steel, tempered steel, stainless steel, WC Co, WC-lined steel and bearing steel. It has been found that alloying occur at a significant higher rates in the flat-ended vial than in the round-ended container [1].

2.3.2.3 Milling Speed and Time:

The Faster the mill rotates the higher would be the energy input into the powder. There are certain limitations on the maximum speed. For example, in a conventional ball mill increasing the speed of rotation will increase the speed with which the balls move. Above a critical speed, the balls will be pinned to the inner walls of the vial and do not fall down to exert any impact force. Therefore, the maximum speed should be just below this critical value so that the balls fall down from the maximum height to produce the maximum collision. Another limitation to the maximum speed is that at high speeds, the temperature of the vial may increase. This may be advantageous in some cases where diffusion is required to promote homogenization and alloying in the powders. But, in some cases, this elevated temperature may be a disadvantage because it accelerates the transformation process and results in the decomposition of supersaturated solid solutions or other metastable phases formed during milling. Additionally, the high temperatures generated may also contaminate the powders [1].

The time is so chosen as to achieve a steady state between the fracturing and cold welding of the powder particles. The times required vary depending on the type of mill used, the speed of milling, the ball-to-powder ratio, and the temperature of milling. Contamination in powder increases with increase in time of milling.

2.3.2.4 Grinding Medium:

Grinding medium are hardened chromium steel, tempered steel, stainless steel, WC Co and bearing steel. The density of the grinding medium should be high enough so that the balls create enough impact force on the powder.

2.3.2.5 Ball to Powder Ratio:

The ratio of the weight of the balls to the powder (BPR), sometimes referred to as charge ratio (CR), is an important variable in the milling process. The BPR has a significant effect on the time required to achieve a particular phase in the powder being milled. The higher the BPR, the shorter is the time required. At a high BPR, because of an increase in the weight proportion of the balls, the number of collisions per unit time increases and consequently more energy is

transferred to the powder. A ratio of 10:1 BPR is most commonly used while milling the powder in a small capacity mill.

2.3.2.6 Milling Atmosphere:

The major effect of the milling atmosphere is on the contamination of the powder. Therefore, the powders are milled in containers that have been either evacuated or filled with an inert gas such as argon or helium.

2.3.2.7 Temperature:

The temperature of milling is another important parameter in deciding the constitution of the milled powder. Since diffusion processes are involved in the formation of alloy phases irrespective of whether the final product phase is a solid solution, intermetallic, nanostructure, or an amorphous phase.

2.4 Production of Alloy Powder:

The actual process of MA starts with mixing of the powders in the right proportion and loading the powder mix into the mill along with the grinding medium. This mix is then milled for the desired length of time until a steady state is reached when the composition of every powder particle is the same as the proportion of the elements in the starting powder mix.

2.5 Mechanism of Milling:

During high-energy milling the powder particles are repeatedly flattened, cold welded, fractured and rewelded. Whenever two balls collide, some amount of powder is trapped in between them. The force of the impact plastically deforms the powder particles leading to work hardening and fracture [6]. The new surfaces created enable the particles to weld together and this leads to an increase in particle size. A broad range of particle sizes develops, with some as large as three times bigger than the starting particles. The composite particles at this stage have a characteristic layered structure consisting of various combinations of the starting constituents. With continued deformation, the particles get work hardened and fracture by a fatigue failure mechanism and/or by the fragmentation of fragile flakes. Fragments generated by this mechanism may continue to reduce in size in the absence of strong agglomerating forces. At this

stage, the tendency to fracture predominates over cold welding. Due to the continued impact of grinding balls, the structure of the particles is steadily refined, but the particle size continues to be the same. Consequently, the inter-layer spacing decreases and the number of layers in a particle increase [6].

After milling for a certain length of time, steady-state equilibrium is attained when a balance is achieved between the rate of welding, which tends to increase the average particle size, and the rate of fracturing, which tend to decrease the average composite particle size. Smaller particles are able to withstand deformation without fracturing and tend to be welded into larger pieces, with an overall tendency to drive both very fine and very large particles towards an intermediate size [6]. At this stage each particle contains substantially all of the starting ingredients, in the proportion they were mixed together and the particles reach saturation hardness due to the accumulation of strain energy. The particle size distribution at this stage is narrow, because particles larger than average are reduced in size at the same rate that fragments smaller than average grow through agglomeration of smaller particles. During MA, heavy deformation is introduced into the particles. This is manifested by the presence of a variety of crystal defects such as dislocations, vacancies, stacking faults, and increased number of grain boundaries. The efficiency of particle size reduction is very low, about 0.1% in a conventional ball mill. The efficiency may be somewhat higher in high-energy ball milling processes, but is still less than 1%. The remaining energy is lost mostly in the form of heat, but a small amount is also utilized in the elastic and plastic deformation of the powder particles [6].

2.6 Advantages of Mechanical Alloying:

- The most significant applications seem to be about 350t of ODS materials, 200t of solder alloy, and 5t of PVD target (Cr–V) alloys per year.
- The use of mechano chemical reactions in producing pure metals, alloys and compounds, dental filling alloys, catalyst materials, inorganic pigments and fertilizers.

2.7 Disadvantages of Mechanical Alloying:

- The industrial applications of MA have been few.
- Powder contamination appears to be a serious problem during MA.

2.8 Definition of the Problem:

The problems like delayed hydride cracking (DHC) and high temperature creep (decrease the life time of the cladding material) were not solved completely. These can be limited by dispersion of some second phase nanoparticles for developing ultrahigh strength zirconium alloys by choosing the correct correlation between the different materials [14].

A major concern in the processing of nanoparticles by MA is the nature and amount of impurities that contaminate the milled powder. Contamination can arise from several sources, including

- Impurities in starting powders,
- Vials and grinding media,
- milling atmosphere, and
- Control agents added to the powders.

During MA the powder particles become trapped between the grinding medium and undergo severe plastic deformation; fresh surfaces are created because of the fracture of the powder particles. Collisions occur between the grinding medium and the vial and among the grinding balls. All of these effects can cause deterioration of the grinding medium and vial, resulting in the incorporation of these impurities into the powder. The extent of contamination increases with increasing milling energy and milling time .Various attempts have been made to minimize powder contamination during MA [15].

CHAPTER 3

EXPERIMENTAL DETAILS

3. Experimental Details:

This chapter contents a brief description of sample history. Zr-based alloy sample (Fe-30-Ni-20-Mo-4 TiO_2-2-Zr-44) (all are in wt. %) were synthesized by mechanical alloying and have been used for the present study. After the description of sample history, mechanical alloying, compaction and sintering, equipment and techniques utilized for characterization of the alloys have been systematically narrated.

3.1 Sample History:

The amounts (wt.%) of Zr, Fe, Ni, Mo and TiO_2 above 99% purity with particle size about 50- 150 μm are shown in Table 1, were subjected to milling under inert atmosphere using a planetary ball mill. Preparation ball mill vial was filled with 11g of zirconium powder, 7.5g of Iron powder, 5g of Nickel powder, 1g of molybdenum powder, 0.5g of TiO_2in the weight percentages of 44, 30, 20 , 4 and 2 respectively. The all elemental powders were mixed and wet milled for 20 h with toluene as liquid medium because it helps in reducing the agglomeration of powders during milling and preventing oxidation on milled powders. Actually, toluene gets adsorbed on the surface of the powder particles and minimizes cold welding between powder particles and thereby inhibits agglomeration.

Table 3.1: Composition of powder blend

Zr (wt %)	Fe (wt %)	Ni (wt %)	Mo (wt %)	TiO_2 (wt %)
44	**30**	**20**	**4**	**2**

3.2 Mechanical Alloying and Process Parameters:

In a planetary ball mill, the elemental powders were subjected to milling which is operated at 300 rpm using harden steel container (500 ml) and harden steel balls (10 mm diameter) to produce Zr-base alloy milled powder. The weight ratio of balls to mixed powder was 10:1. The milling was performed in manual mode with 30 minutes interval. For property analysis (XRD and SEM) of the Zr based alloy of given systems we had taken the samples with

the time stages like 0 h, 1 h, 5 h, 10 h, 15 h and 20 h. the details of milling parameters are listed at Table 2.

Fig 3.0 Planetary ball mil

Table 3.2: Milling process parameters

Parameters	Operating condition
Type of mill	Planetary mill
Milling container	High strength Chrome steel
Milling speed	300rpm
Grinding medium	Toluene
Ball diameter	10 mm
Balls to powder wt. ratio	10:1
Milling time	20hr
Weight of powder	25g

3.3 Compaction and Sintering:

The consolidation of the milled powder at 20 h was cold compacted using a hydraulic compressor with a load of 10 tones to form round disk specimens of 2.7 mm thickness and 13 mm in diameter and followed by conventional sintering carried out at 1400°C in argon atmosphere for 2 hours.

3.4 Characterization of Mechanically Alloyed Powders and Sintered Products:

Milled powders of different stages like 0 h, 1 h, 5 h, 10 h, 15 h and 20 h and sample sintered at 1400°C were characterized by X-Ray Diffraction (XRD), scanning electron microscope (SEM) to understand the evolution of different phase during each stage of milling and sintered product. The shape, size and morphology during each stage of milling are optimized by scanning electron microscope (SEM) techniques.

3.4.1 X– Ray Diffraction Analysis:

The purpose of X-ray diffraction (XRD) studies to identity and phase evolution at different hours of milling sample and also after sintering by using a standard diffractometer (*Philips* X'Pert MPD) was shown in Fig. 3.1 with Ni-filtered Cu K_α radiation ($\lambda = 0.154051$ nm). The X-ray source was operated at a voltage of 40 kV and current of 35 mA. The diffraction angle was varied in the range of 20-100 degrees and the scanning rate was 0.05degree/s. Phillip's X'pert software is used for analyzed of XRD data diffraction patterns. **B**y using Williamson-Hall plot the crystallite size and lattice strain were estimated by measuring the broadening of the X-ray peaks by using Williamson- Hall plot.

Fig. 3.1: X-ray diffractometer

3.4.2 Scanning Electron Microscopy:

A JEOL JSM-6480 LV scanning electron microscope (shown in Fig. 3.2) is utilized for microstructure characterization, morphology and particle size determination. Both the secondary electron (SE) mode and back scattered electron mode (BSE) were used as per the requirement.

Fig. 3.2: Scanning electron microscope.

3.4.3 Hardness Measurement:

The mechanical properties of the alloy micro-hardness measurement were carried out in a micro-hardness tester. Vickers micro hardness tester (shown in Fig. 3.3) is used for hardness study of compact and sinter samples. The sample preparation was done primarily by using 1/0, 2/0, 3/0 and 4/0 emery papers there after cloth polishing was done. Hardness was measured on all the samples using Vickers hardness tester. 10 kg loads for dwell time of 10 seconds and a square base diamond pyramid indenter with an included angle of 360° between the faces were used during hardness measurement. The indenter's shape results in square shape on the surface of the specimen. Then, length of the diagonals of the square was measured through a microscope fitted with an ocular micrometer. Machine itself displays the hardness value in Vickers Pyramid Number (HV). At least 4 readings were taken sintered sample each sample.

Fig 3.3: Micro hardness tester

CHAPTER 4

RESULTS AND DISCUSSIONS

4 Results and Discussion:

4.1 X-ray diffraction study:

Fig. 4.0 shows the series of XRD patterns of (Fe-30-Ni-20-Mo-4 TiO_2-2-Zr-44) (all are in wt. %) alloy subjected to milling at various milling time 0h, 1h, 5h, 10h, 15h and 20h. After 5 h of milling, it shows the alloying elements are making complete solid solution with Zr matrix. It reveals that the nanocrystalline phases were formed at 5 h of milling which the same trends were found at 10 h, 15 h and 20 h respectively. After 15 h of milling, all peaks are disappeared except the present of three broaden peaks of Zr matrix and further 20 h of milling it shows complete solid solution with Zr matrix. The originally sharp diffraction lines of Zr, Fe, Ni and Mo gradually become broader and their intensity decreases with increasing milling time. This is due to all elements goes into the solid solution in Zr matrix. Therefore, a gradual refinement and alloying of the elements is observed with increasing the milling time as revealed by the appearance of broad peaks and by a decrease of intensity of the diffraction peaks related to the elemental powders.

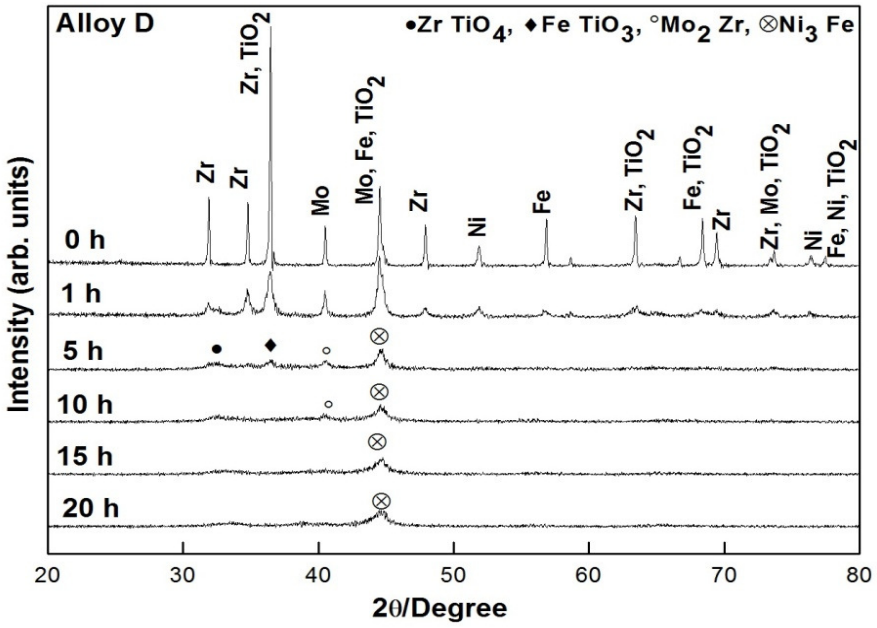

Fig. 4.0 XRD patterns of mechanical alloyed powders of $Zr_{44}Fe_{30}Ni_{20}Mo_5$ at different milling time (0 h, 1 h, 5 h, 10 h, 15 h and 20 h)

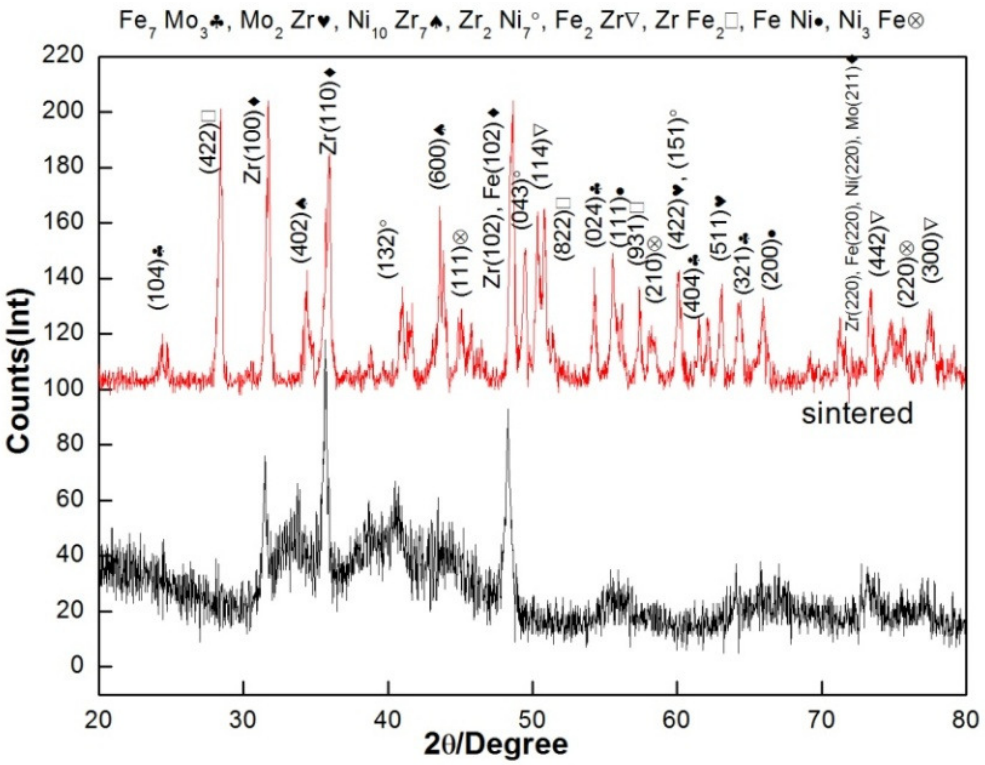

Fig. 4.1: XRD patterns of sintered product and mechanical alloyed powder at 20 h

Fig. 4.1 shows the formation of different phases like Fe_7Mo_3, Mo_2Zr, $Ni_{10}Zr_7$, Zr_2Ni_7, Fe_2Zr, $ZrFe_2$, FeNi and Ni_3Feafter the sintering at 1400°C. Destabilization of the crystalline phase is thought to occur by the accumulation of structural defects such as vacancies, dislocations, grain boundaries, and anti-phase boundaries. The continuous decrease in grain size (and consequent increase in grain boundary area) and a lattice expansion would also contribute to the increase in free energy of the system. This leads to formation of amorphous and intermetallic phase [12, 13].

4.2 Crystallite Size and Lattice Strain Calculation during Mechanical Alloyed Powders:

The measurement of crystallite size and lattice strain of milled powders (0 h, 1 h, 5 h, 10 h, 15 h and 20 h) were calculated by using William –Hall equation. Various factors like instrumental error, crystallite size and microstrain are the reason for the peak broadening of Zr.

Scherer's formula: (the line broadening due to the crystallite size)

$$\beta_t = \frac{0.9\lambda}{D\cos\theta}$$

Where

'D' - Crystallite size,

'λ' - wave length of X-Ray (0.1541 nm),

'β_t' - FWHM (full width at half maximum due to crystallite size)

'θ' - the diffraction angle.

Wilson formula: (the line broadening due to microstrain)

$$\beta_s = 4\varepsilon\tan\theta$$

Where

'ε' - the root mean square value of microstrain,

' β_s' -FWHM (full width at half maximum due to microstrain)

'θ' - the diffraction angle.

In determining the crystallite size and lattice strain, it is considered that the line broadening due to the crystallite size and microstrain are independent of each other and both have a Cauchy like profile i.e. the observed line breadth is equal to the linear sum 'β_t' and β_s'.

$$i.e.\ \beta = \beta_t + \beta_s$$

$$i.e.\ \beta\cos\theta = \frac{0.9\lambda}{D} + 4\varepsilon\sin\theta$$

The above equation is called Williamson-Hall equation. $'\beta\cos\theta'$ is plotted against '$4\sin\theta'$ for determining the crystallite size and the lattice strain . On plotting, the slope of the straight line obtained will give the lattice strain and the crystallite size can be determined from the intercept.

Table 4.1: Calculated average crystallite size and lattice strain by using William –Hall equation of the current alloy at different stage of milling (0 h, 1 h, 5 h, 10 h, 15 h and 20 h)

Milling Time	2Ɵ	βCos Ɵ	4Sin Ɵ	Average. Crystallite Size (nm)	Lattice Strain (%)
0 h	34.74	0.091	1.194	1.27	0.18
	44.55	0.154	1.516		
	47.89	0.109	1.623		
1 h	34.74	0.274	1.194	0.63	0.31
	44.55	0.177	1.516		
	47.89	0.263	1.623		
5 h	34.74	0.549	1.194	0.46	0.33
	44.55	0.442	1.516		
	47.89	0.178	1.623		
10 h	34.74	1.099	1.194	0.39	1.2
	44.55	0.708	1.516		
	47.89	0.170	1.623		
15 h	34.74	0.248	1.194	0.43	1.6
	44.55	0.768	1.516		
	47.89	0.311	1.623		
20 h	34.74	0.261	1.194	0.35	2.1
	44.55	0.960	1.516		
	47.89	0.09	1.623		

Fig 4.2 shows that the crystallite size of current alloy decreases gradually with increase in milling time from 0 h to 20 h. Again, from Fig. 4.3 shows that lattice strain increase gradually with increase in milling time. This is because there is a tendency of the particle size to reach an equilibrium value as milling time increases. Actually steady state equilibrium is reached when there is a balance between the rate of welding, which tends to increase the particle size, and the rate of fracturing, which tends to decrease the average composite particle size. Crystal refinement due to mechanical milling increases the strain in the lattice. Similar kinds of results were established by several researchers [1, 6].

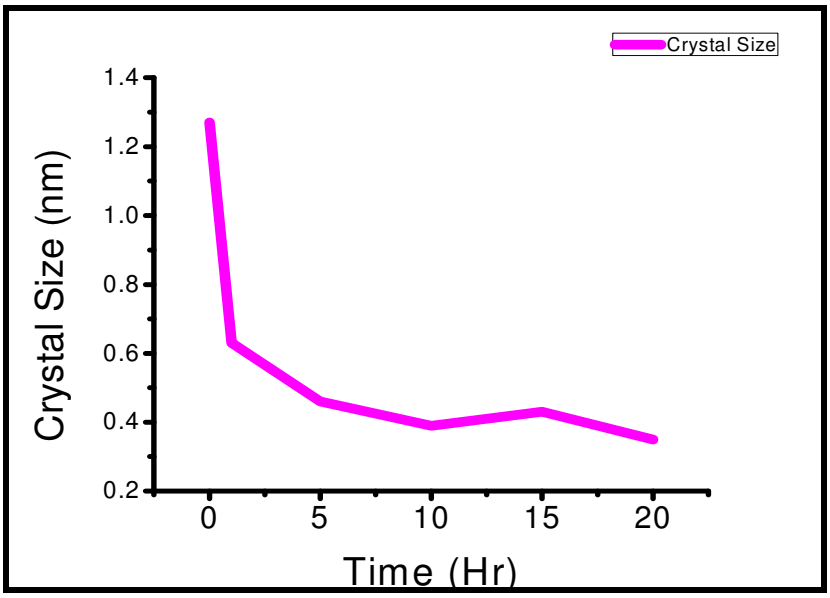

Fig.4.2: Crystallite size is the function of milling time.

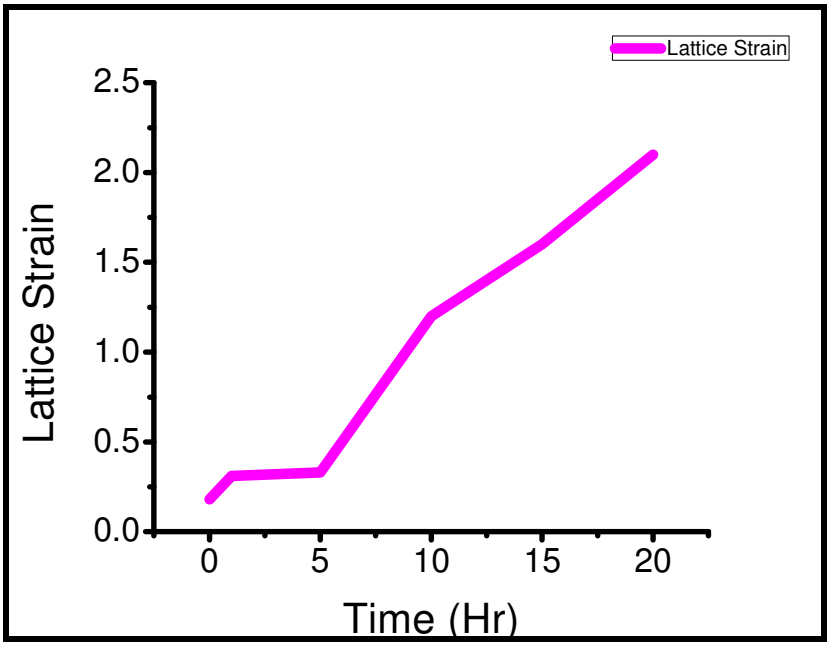

Fig.4.3: Lattice strain is the function of milling time

4.3 SEM Analysis of Mechanical Alloyed Powders:

Figs. 4.4 (a-e) show the Scanning electron micrographs of milled powders at (a) 0 h, (b) 1h, (c) 5h, (d) 15 h and (e) 20 h, respectively. It reveals that as milling time increase the particle size of the alloy gradually decreases to the range of 20 μm to 1.0 μm. It can be seen that the structure is relatively finer and homogeneous with increasing milling time. It can be found that coarse grains milling time from 0-1 h, with visible polyhedron profile in Fig. 4.4(b), and the grain size of which changes from 1to 15μm. from Fig. 4.4 (c) to 4.4(e), the grain size is relatively small and distributes more uniformly.

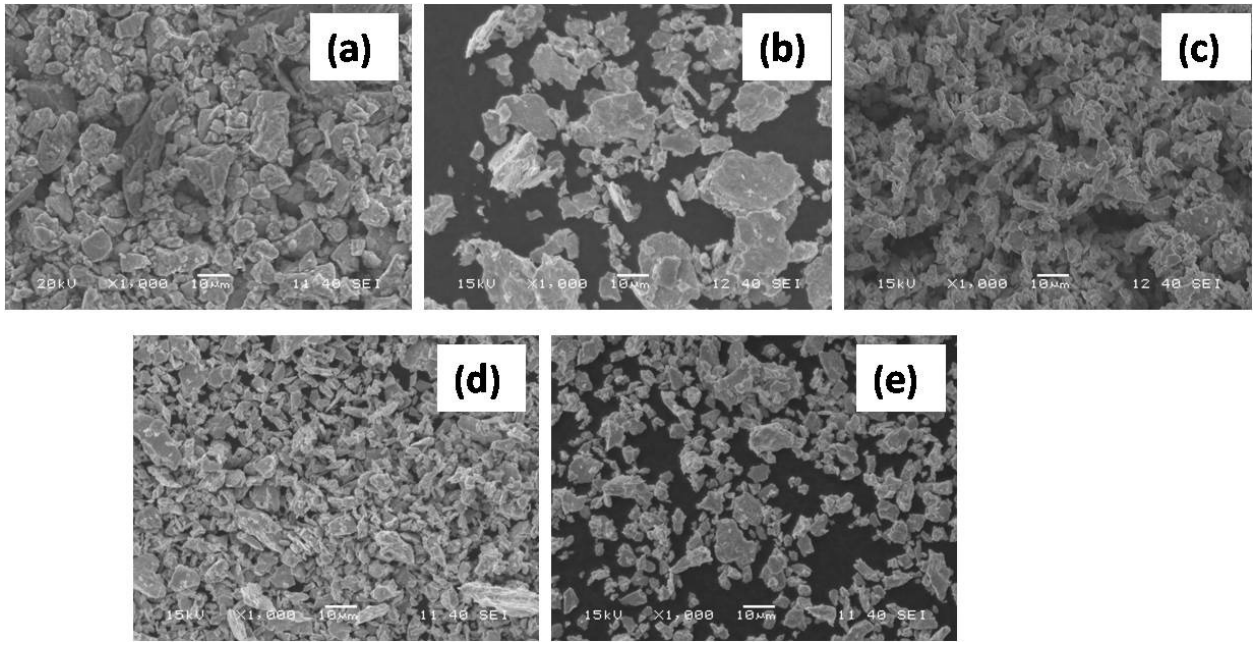

Fig. 4.4: Scanning electron micrographs of milled powders at (a) 0 h, (b) 1h, (c) 5h, (d) 15 h and (e) 20 h respectively.

4.4 Hardness Study:

The hardness of sintered sample is summarized in Table 4.2. It is predict that the hardness of current alloy is extremely high (710 HV) which is 1-1.2 times higher than that of literature value [27]. The enhancement of hardness is due to the uniform dispersion of TiO_2 in the Zr matrix. It follows the dispersion hardening strengthening mechanism. Densification of

the green compact by sintering leads to the distortion of component. This may be the cause of increasing the strength of the sintered sample. Strength of the alloy increased due to uniform dispersion of oxide particles. The mechanical strength of the present alloys can be interpreted by various strengthening mechanisms such as dispersion hardening, solid solution hardening and grain refinement (Hall–Petch effect).

Table 4.2 : Hardness values of sintered alloy and literature

Sample	**Avg. Hardness (HV)**
Sintered sample	710
Literature value [27]	550

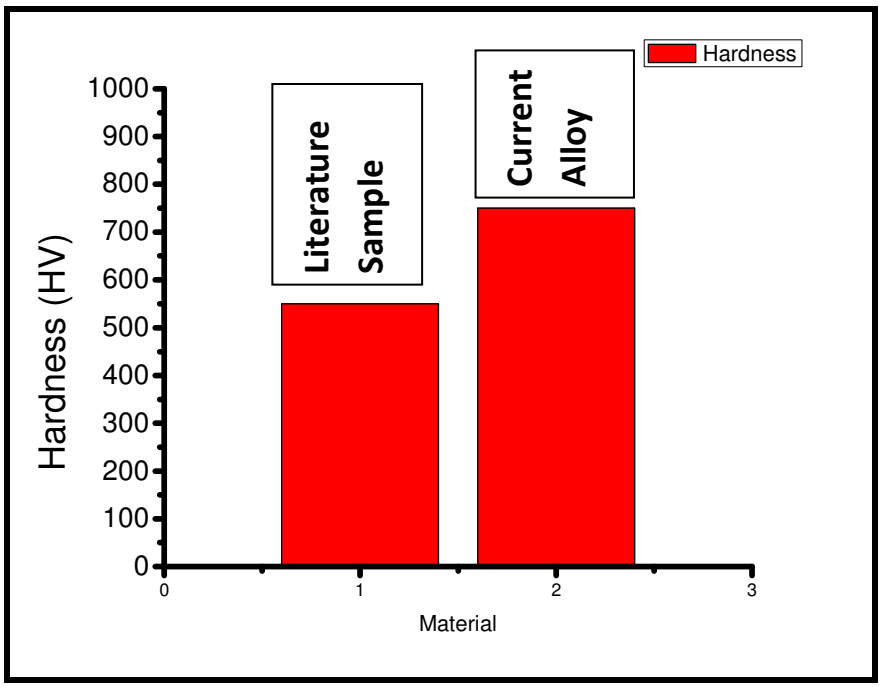

Fig 4.5: Comparison of hardness value in both literature and current alloy

4.5 Discussions:

After 20 h of milling, the elementals go to complete solid solution in the Zr matrix was observed Fig. 4.0. It shows the peaks are broadening with increasing milling time which mainly the increase of lattice strains. With increase in milling time particle size decreases in general and is confirmed by SEM. Particle size was decreased with increasing milling time up to 15 h of milling and then again it increases size at 20 h of milling; this is due to re-welding of the powder particles. Ultra high strength is obtained because of dispersion of nano-TiO_2 phase in Zr matrix. The mechanical strength mainly hardness of the present alloy can be interpreted by various strengthening mechanisms such as dispersion hardening, solid solution hardening and grain refinement (Hall–Petch effect). There is chance of grain coarsening during sintering which can't be neglected. In spite of that strengthening effect on the alloy due to uniform dispersion of nano-TiO_2 in Zr matrix and solid solution effects would dominate over grain refinement. Mechanically alloyed materials are strong both at room and elevated temperatures. The elevated temperature strength is derived from more than one mechanism. First, the uniform dispersion (with a spacing of ~100nm) of very fine (5–50nm) oxide particles ofTiO_2 which are stable at high temperatures, inhibit dislocation motion in the metal matrix, and increase the resistance of the alloy to creep deformation. Another function of the dispersoid particles is to inhibit the recovery and recrystallization processes, which allow a very stable grain size to be obtained. These large grains resist grain rotation during high-temperature deformation. The very homogeneous distribution of alloying elements during MA gives both the solid solution strengthened and precipitation-hardened alloys more stability at elevated temperatures and overall improvement in properties.

CHAPTER 5

SUMMARY AND CONCLUSION

5 Summary and Conclusion:

The carefully analysis of experiments and results the following conclusions can be drawn:

- It is possible to synthesis of Zr- alloy (Fe-30-Ni-20-Mo-4- TiO_2-2-Zr-44) (all are in wt. %) dispersed TiO_2 (2 wt %) by mechanical alloying.
- Particle size was decreased with increasing milling time during 1h to 15 h of milling and then increased at 20 h of milling; this was due to re-welding of the powder particles.
- It is found that the particle size of alloy powder synthesized by mechanical alloying goes to the nanometric range which is confirmed by XRD and SEM analysis.
- Crystallite size decreases and the lattice strain increases with increase in the extent of milling.
- The Zr- alloy (Fe-30-Ni-20-Mo-4 TiO_2-2-Zr-44) (all are in wt. %) shows the improvement of hardness value (710 HV) which is 1-1.5 times higher than that of the conventional Zircaloy (~500 HV).
- Enhancement of the hardness of the current alloy is due to the uniform dispersion of nano-TiO_2 in Zr matrix.

Reference:

1. C. Suryanarayana: 'Mechanical alloying and milling', Progress in Materials Science, 2001, 46, 1-184.
2. M. Jurczyk: 'Nanocrystalline materials for hydrogen storage', Journal of optoelectronics and advanced materials, 2006, 8, 418 – 424.
3. Ludwig Schultz: 'Formation of amorphous metals by mechanical alloying', Material science and engineering, 1988, 97, 15-23.
4. A. W. Weeber and H. Bakker: 'Amorphous Transition Metal-Zirconium Alloys Prepared by Milling', Materials Science and Engineering, 1988, 97, 133-135.
5. A. R. Yavari and P. J. Desre: 'Amorphization by mechanical alloying and by solid-state reaction: Similarities and differences', Materials Science and Engineering, 1991, A 1.74, 1315-1322.
6. C. Suryanarayana, E. Ivanov, and V.V. Boldyrev: 'The science and technology of mechanical alloying', Materials Science and Engineering, 2001, A304–306,151–158.
7. A. Grabias, D. Oleszak and M. Pekala: 'Structure and magnetic properties of the Zr30Fe35Ni35 alloy formed by mechanical alloying', Rev.Adv.Mater.Sci. 2008, 18, 379-383.
8. V. Kapaklisa, S. Baskoutasb and C. Politisac: 'Glass forming ability of bulk and mechanically alloyed Zr55Cu19Ni8Al8Si5Ti5 amorphous alloys', Journal of Optoelectronics and Advanced Materials, 2003, 5, 1255 – 1258.
9. A. Al-Hajry: 'Fast amorphization reaction in ZrNi system prepared by mechanical alloying', Materials Research Bulletin, 2000, 35, 1989–1998.
10. S. Scudino, D.J. Sordelet and J. Eckert: 'Devitrification of mechanically alloyed Zr-Ti-Nb-Cu-Ni-Al glassy powders studied by time-resolved x-ray diffraction', Rev.Adv.Mater.Sci. 2008, 18, 221-224.

11. Pee-Yew Lee, Carl C. Koch: 'Microstructural evolution of Ni40Zr60 alloy during early stage of mechanical alloying of intermetallic compounds NiZr, and NiIIZr', Materials Chemistry and Physics, 1994, 38, 199-202.
12. . L. Schultz: 'Glass formation by mechanical alloying', Journal of the Less-Common Metals, 1998, 145, 233 – 249.
13. . J. Eckert, L. Schultz, and I. Urban: 'Glass-forming ranges in transition metals & alloys prepared by mechanical alloying', Journal of the Less-Common Metals, 1998, 145, 283 – 291.
14. Delin Pengy, Jun Shen, Jianfei Sun and Yuyong Chen: 'Kinetic Characteristic of Hydrogenation Zr-Ti-Cu-Ni-Be Bulk Amorphous Alloys', J. Mater. Sci. Technol., 2004, 20, 20.
15. Javed Iqbal Akhter, Haifeng Zhang Huand Zhuangqi Muhammad Iqbal: 'Effect of Minor Alloying on Crystallization Behavior and Thermal Properties of Zr64.5Ni15.5Al11.5Cu8.5 Bulk Amorphous Alloy', J. Mater. Sci. Technol., 2011, 27, 534-538.
16. Eunji Hong, David C. Dunand, and Heeman Choe: 'Hydrogen-induced transformation super plasticity in zirconium', international journal of hydrogen energy, 2010, 35, 5708-5713.
17. S. Bera and I. Manna: 'Polymorphic phase transformation in Ti50Zr50 binary alloy by mechanical alloying', Materials Science and Engineering, 2006, A 417, 110–113.
18. $(FeAl3)_{1-x}$ Zr_x amorphous alloys prepared by mechanical alloying Yifang Ouyanga,_, Hongmei Chena, Xiaping Zhonga, Yong Dub, Physica B 391 (2007) 380–384
19. O. Held, J.P. Braganti and F.A. Kuhnast: 'Calorimetric and structural analysis of the new phase Al Ni Zr 33 16 51 produced by direct synthesis and mechanical alloying', Journal of Alloys and Compounds, 1999, 290, 197–202.
20. Y.H. Jeong, J.Y. Park, H.G. Kim, J. T. Busby, E. Gartner, M. Atzmon, G. S. Was,R.J. Comstock, Y.S. Chu, M. Gomes da Silva, A. Yilmazbayhan and A.T. Motta: 'Corrosion of Zirconium-based Fuel Cladding Alloys in Supercritical Water', TMS (The Minerals, Metals & Materials Society), 2005
21. R. Krishnan and M. K. Asundiproc: 'Zirconium alloys in nuclear technology', Indian Acad,Sci. (Engg. Sci., 1981, 4, 41-56.

22. Bing K. Yen: ‘X-ray diffraction study of mechanochemical synthesis and formation mechanisms of zirconium carbide and zirconium silicides’, Journal of Alloys and Compounds, 1998, 268, 266–269.
23. A. AL-Hajry, M. AL-Assiri and N. Cowlam: ‘X-ray and neutron diffraction studies of the amorphous ZrPd alloys, J. Phys. Chem Solids, 1998, 59, 1499-1505
24. O. J. Dura, E. Bauer, L. Vazquez and M. A. Lopez de la Torre: ‘Depressed thermal conductivity of mechanically alloyed nanocrystalline 10 mol%yttria-stabilized zirconia’, Journal of Physics D: Applied Physics, 2010, 43, 10.
25. Z. Zhao,M. Blat-Yrieix,J.-P. Morniroli,A. Legris,L. Thuinet,Y. Kihn,A. Ambard andL. Legras: ‘Characterization of Zirconium Hydrides and Phase Field Approach to a Mesoscopic-Scale Modeling of Their Precipitation’, Journal of ASTM International, 2008, 5, 3.
26. M. Sherif El-Eskandarany: ‘Mechanical alloying for fabrication of advanced engineering materials’, NOYES PUBLICATIONS Norwich, New York, U.S.A. 2001.
27. S. Janaa, U. Ramamurtya, K. Chattopadhyaya, Y. Kawamurab: ‘Subsurface deformation during Vickers indentation of bulk metallic glasses’ Materials Science and Engineering A 375-377, 2004, 1191–1195,